We are IntechOpen,
the world's leading publisher of Open Access books
Built by scientists, for scientists

6,900
Open access books available

185,000
International authors and editors

200M
Downloads

154
Countries delivered to

Our authors are among the

TOP 1%
most cited scientists

12.2%
Contributors from top 500 universities

BOOK CITATION INDEX
CLARIVATE ANALYTICS
INDEXED

WEB OF SCIENCE™

Selection of our books indexed in the Book Citation Index
in Web of Science™ Core Collection (BKCI)

Interested in publishing with us?
Contact book.department@intechopen.com

Carbon Nanotubes in Passive RF Applications

Ahmed M. Attiya and Majeed A. Alkanhal
King Saud University, Electrical Engineering Dept
Saudia Arabia

1. Introduction

Carbon nanotubes are characterized by unique electrical properties which make them good candidates for different applications in electronics and electrical engineering. In this chapter we focus mainly on electrical properties of single wall conducting carbon nanotubes in high frequency, electromagnetic waves interaction with carbon nanotubes and the possible passive RF applications. The term "high frequency" here refers to the frequency band from gigahertz to terahertz. This chapter starts from microscopic view by discussing electrodynamics of carbon nanotubes to show the mechanism of time varying electromagnetic field interaction with carbon nanotubes (Slepyan *et al.*, 1999; Slepyan *et al.*, 2008; Mikki & Kishk 2008). Based on these electrodynamics properties, an equivalent dynamic surface conductivity is developed to represent a macroscopic view for the interaction of high frequency electromagnetic fields with carbon nanotubes (Hanson, 2005). This equivalent surface conductivity of carbon nanotube is characterized by complex value with negative imaginary part. This negative imaginary part represents an inductive effect in carbon nanotubes. This inductive effect is due to chiral property of the electric current flow along the carbon nanotube (Slepyan *et al.*, 1998; Miyamoto *et al.* 1999). This inductivity has a significant effect on reducing the wave velocity of electromagnetic wave propagation along carbon nanotube. This wave velocity reduction corresponds to decreasing the wavelength. This property is quite important in passive RF applications like passive circuits and antennas, since the dimensions of these applications depend mainly on the wave length (Slepyan *et al.*, 1999; Slepyan *et al.*, 2008; Attiya, 2009).

Based on the macroscopic surface conductivity of carbon nanotube, the problems of electromagnetic fields interaction with carbon nanotubes can be presented in similar ways to conventional problems related to cylindrical structures with finite surface conductivity. In this way the problem of carbon nanotube antennas can be presented as an electric field integral equation problem which can be treated numerically by method of moments (Hanson, 2005; Hao & Hnason, 2006). Similarly, the problem of surface wave propagation along carbon nanotubes can be presented as a boundary value problem where the difference between the tangential magnetic fields on the two sides of the wall of the carbon nanotube would equal the induced current on the wall of the carbon nanotube. This induced current depends on the tangential electric field along the carbon nanotube and the surface conductivity. This boundary value problem is solved to obtain the field distribution and the complex propagation constants of the surface wave modes propagating along carbon

nanotube (Slepyan *et al.,* 1999; Shuba *et al.* 2007; Slepyan *et al.,* 2008; Attiya, 2009). This surface wave propagation is characterized by highly attenuation coefficient at microwave frequency band. This property makes carbon nanotubes are not suitable for antenna design. However, this high attenuation property is more suitable for other applications which are based on absorbing or attenuating electromagnetic waves like transparent electromagnetic shielding (Xu *et al.,* 2007) and microwave heating in biomedical applications (Mashal *et al.,* 2010). On the other hand, at higher frequency bands in the range above 100 GHz, this attenuation coefficient is decreased and carbon nanotubes can be a good candidate to design low loss antenna structures of much smaller size compared with operating free space wave length (Huang *et al.* 2008 & Attiya, 2009).

Another common approach for simulating electromagnetic wave propagation along carbon nanotube is based on electron fluid model (Burke, 2002; Chiariello *et al.,* 2006a; Miano & Villone 2006). This model is more suitable for simulating transmission line sections of carbon nanotubes. In this case the inductive effect of current flow along the carbon nanotube transmission line is modeled as an additional kinetic inductance in the equivalent circuit model of this transmission line (Burke, 2002; Chiariello *et al.,* 2006b; Miano & Villone 2006; Maffuci *et al.* 2008; Maffuci *et al.* 2009). This kinetic inductance has much greater value than the conventional magnetic inductance of conventional transmission lines. This increase in the total inductance introduces two main effects; decreasing the wave velocity along the line and increasing the characteristic impedance of the line. To improve the properties of carbon nanotube transmission lines, bundles of carbon nanotube are used instead of a single carbon nanotube (Plombon *et al.,* 2007; Rutherglen *et al.* 2008). Extensive studies are presented in literature about the possibility of using carbon nanotube bundles as interconnects in high speed integrated circuits (Massoud & Nieuwoudt, 2006; Naeemi & Meindl, 2009).

Recently, another new approach is discussed for solving the interaction between Maxwell's equation and Schrödinger equation numerically by using finite difference method to obtain electromagnetic field interaction with nanodevices like those which are based on carbon nanotubes (Pierantoni *et al.;* 2008, Pierantoni *et al.;* 2009 & Ahmed *et al.;* 2010). This method is based on space-time discretization. The electromagnetic source is modeled by means of time dependent vector and scalar potentials which are added to the quantum potential profile of the carbon nanotube. Then Schrödinger equation is solved by using a finite difference scheme to obtain the wave equation of electron flow along the carbon nanotube.

The aim of the present chapter is to introduce to the reader an updated view for the problems of electromagnetic field interaction with carbon nanotube with emphasis on the possible passive RF applications. Section 2 presents the electrodynamics of carbon nanotube and the concept of equivalent macroscopic surface conductivity. Section 3 presents the electron fluid model of carbon nanotube and how it can be used to obtain equivalent circuit parameters of carbon nanotube transmission lines. Section 4 presents finite difference time domain method as numerical technique for studying electromagnetic interaction with carbon nanotubes. Section 5 presents detailed analysis of surface wave propagation along carbon nanotubes. Section 6 introduces the electric field integral equation formulation of carbon nanotube antenna and presents sample results for this problem. Section 7 discusses the possibility of using carbon nanotubes in some passive RF circuits. Finally, Section 8 introduces some possible applications of carbon nanotubes based on their absorbing properties in microwave frequencies.

2. Dynamic conductivity of carbon nanotubes

Dynamic conductivity of a carbon nanotube represents a macroscopic quantity relating the disturbance of electron flow along the nanotube due to an incremental temporal variation in the applied electric field along it. For conventional carbon nanotube structures, the length of the nanotube is much greater than its circumference. Thus, for most practical cases, it is assumed that the equivalent current along the surface of the nanotube is transversely symmetric and parallel to the axis of the nanotube. In the following analysis the geometry of the nanotube is assumed to be presented in cylindrical coordinate system, where the axis of the nanotube lies along the z-axis. Thus, the proposed dynamic conductivity in this case is the relation between the surface current density J_z and the applied electric field E_z.

The applied field is presented as a time harmonic propagating wave along the axis of the nanotube as follows:

$$E_z(z,t) = \mathrm{Re}\left(E_z^0 e^{j\omega t - \gamma z} \right) \tag{1}$$

where E_z^0 is the amplitude of the incident field, ω is the angular frequency and γ is the complex propagation constant along the nanotube. This complex propagation constant is discussed in detail in Section 5. However, in the present case, the dependence of the electric field on z can be assumed to be constant by taking the limit where an incremental length of the nanotube is considered. Thus, for a very small part of the nanotube, the incident field is assumed to be $E_z(t) = \mathrm{Re}\left(E_z^0 e^{j\omega t} \right)$.

This applied electric field introduces a disturbance in the electron distribution function along the nanotube. At equilibrium, the electron distribution function is given by:

$$F(\mathbf{p}) = 1 / \left[1 + \exp\left(\mathrm{E}(\mathbf{p}) / k_B T \right) \right] \tag{2}$$

where $\mathbf{p} = p_z \mathbf{a}_z + p_\varphi \mathbf{a}_\varphi$ is the electron's two-dimensional quasi-momentum, k_B is Boltzman constant, T is the absolute temperature and $\mathrm{E}(\mathbf{p})$ is the electron energy with respect to the Fermi level in the lattice of the carbon nanotube. By applying an axial time harmonic electric field on the nanotube, this distribution function along an incremental length is modified as follows:

$$f(\mathbf{p},t) = F(\mathbf{p}) + \mathrm{Re}\left(\delta f\, e^{j\omega t} \right) \tag{3}$$

This dynamic distribution function is governed by Boltzman kinetic equation (Dressel & Grüner, 2003). By taking into consideration that the problem is transversely symmetric, the applied field is only along the axis of the nanotube one can obtain Boltzman kinetic equation for the carbon nanotube as follows:

$$\frac{\partial f}{\partial t} + eE_z \frac{\partial f}{\partial p_z} + \mathrm{v}_z \frac{\partial f}{\partial z} = \frac{1}{\tau}\left(F - f \right) \tag{4}$$

where τ is the electron relaxation time in the lattice of the carbon nanotube, $\mathrm{v}_z = \partial \mathrm{E}(\mathbf{p}) / \partial p_z$ is axial electron velocity and $\mathrm{E}(\mathbf{p})$ is the electron energy function. This relaxation time is nearly 3 ps in carbon nanotube (Hanson 2006). By applying the time harmonic electric field

and the dynamic distribution function of Equation (3) into Equation (4), one can obtain the incremental disturbance in the distribution function as

$$\delta f = \frac{jeE_z^0}{\omega - jv}\frac{\partial F}{\partial p_z} \qquad (5)$$

where $v = 1/\tau$ is the relaxation frequency and e is the electron charge. The amplitude of the time harmonic current density along the surface of the nanotube can be obtained by using this disturbance function in the electron distribution function as follows:

$$J_z^0 = \frac{2e}{h^2}\iint\limits_{1^{st}BZ} v_z \delta f\, dp_z dp_\phi \qquad (6)$$

where h is Planck's constant. The range of integration in Equation (6) refers to the first Brillouion zone of the carbon nanotube lattice. By inserting Equation (5) into Equation (6), one can obtain a linear relation between the amplitude of the incident time harmonic electric field and the resulting surface current density as follows:

$$J_z^0 = \sigma_{zz}E_z^0 \qquad (7)$$

where the equivalent axial conductivity σ_{zz} is given by

$$\sigma_{zz} = \frac{2e^2}{h^2}\frac{j}{\omega - jv}\iint\limits_{1^{st}BZ}\frac{\partial F(\mathbf{p})}{\partial p_z}\frac{\partial E(\mathbf{p})}{\partial p_z}dp_z dp_\phi = \frac{2e^2}{h^2}\frac{j}{\omega - jv}\iint\limits_{1^{st}BZ}\frac{\partial F}{\partial E}\left(\frac{\partial E(\mathbf{p})}{\partial p_z}\right)^2 dp_z dp_\phi \qquad (8)$$

It should be noted that the azimuth momentum p_ϕ has discrete values in nanotube since electron energy in this case is a periodic function of ϕ. Thus, the double integration in Equation (8) is converted into a finite series of single finite integration.

The key difference between the conductivities of the different types of the carbon nanotube lies in the corresponding electron energy function $E(\mathbf{p})$. This electron energy function depends mainly on the chiral vector of the carbon nanotube. Each chiral vector is a combination of integer multiplications factors, m and n, of the two basis lattice vector for a graphite sheet. For a zigzag carbon nanotube, where the indices of the chiral vector of the carbon nanotube lattice are $m \neq 0$ and $n = 0$ and, The electron energy function is given by:

$$E_{zigzag}(\mathbf{p}) = \pm\gamma_0\sqrt{1 + 4\cos\left(\frac{3bp_z}{h/\pi}\right)\cos\left(\frac{\sqrt{3}bp_\phi}{h/\pi}\right) + 4\cos^2\left(\frac{\sqrt{3}bp_\phi}{h/\pi}\right)} \qquad (9\text{-}a)$$

where $b = 1.42\overset{\circ}{A}$ is the interatomic distance in a graphite sheet, $\gamma_0 \approx 2.7-3.0\,eV$ is the characteristic energy of the graphene lattice and the azimuth momentum in this case is given by:

$$p_\phi = hs/\left(\sqrt{3}mb\right), \qquad s = 1, 2, 3, \dots, m \qquad (9\text{-}b)$$

For the case of an armchair carbon nanotube where the indices of the chiral vector are equal, $m=n$, the electron energy function is given by:

$$E_{armchair}(\mathbf{p}) = \pm\gamma_0\sqrt{1 + 4\cos\left(\frac{3bp_\phi}{h/\pi}\right)\cos\left(\frac{\sqrt{3}bp_z}{h/\pi}\right) + 4\cos^2\left(\frac{\sqrt{3}bp_z}{h/\pi}\right)} \qquad (10\text{-}a)$$

where the azimuth momentum in this case is given by:

$$p_\phi = hs/(3mb), \qquad s = 1,2,3,\dots,m \qquad (10\text{-}b)$$

By inserting Equations (9) and (10) into Equation (8) and evaluating the required integration one can obtain the axial conductivity for both zigzag and armchair carbon nanotubes. For the cases of small values of m (where $m<60$), these integrals can be evaluated approximately in closed forms. Zigzag carbon nanotubes have conducting properties for values of m which are integer multiple of three. In this case, the dynamic conductivity of zigzag carbon nanotube is given by:

$$\sigma_{zz\_zigzag} \approx -j\frac{8\pi\sqrt{3}e^2\gamma_0}{mh^2(\omega - jv)}, \qquad m = 3N, n = 0 \qquad (11\text{-}a)$$

On the other hand, armchair carbon nanotubes are always conductor for all values of m. The dynamic conductivity of armchair carbon nanotube is given by:

$$\sigma_{zz\_armchair} \approx -j\frac{8\pi e^2\gamma_0}{mh^2(\omega - jv)}, \qquad m = n \qquad (11\text{-}b)$$

For a chiral carbon nanotube where $m \neq n$ and $n \neq 0$, the carbon nanotube is conducting if $2m + n = 3N$ where N is an integer value. In this case the dynamic conductivity of the carbon nanotube is given by:

$$\sigma_{zz\_chiral} \approx -j\frac{8\pi\sqrt{3}e^2\gamma_0}{h^2\sqrt{m^2 + mn + n^2}(\omega - jv)}, \qquad 2m + n = 3N \qquad (11\text{-}c)$$

Equation (11) represents the dynamic conductivity for the different types of conducting carbon nanotubes. It should be noted that this conductivity corresponds to a surface conductivity. Thus the unit here is Siemens. It can be noted that these dynamic conductivities are complex values of negative imaginary part while for conventional conductor the conductivity is usually a real part. This negative imaginary part in the conductivity of carbon nanotube corresponds to an additional inductive effect in the mechanism of the electron current flow along it. This inductive effect introduces slow wave propagation along the carbon nanotube as it is discussed in the following section. This slow wave property corresponds to a decrease in the wavelength along the carbon nanotube. Since the dimensions of RF circuits and antennas depend on the electrical length, this reduction in wave velocity along the carbon nanotube is expected to be quite useful for size reductions of RF circuits and antennas.

For the sake of comparison (Hanson 2005) introduced the equivalent surface conductivity of a hollow copper nanotube as:

$$\sigma_{2d\_cu}(\omega) = -j\frac{e^2 N_{e\_cu}^{2d}}{m_e\left(\omega - jv_{cu}\right)} \tag{12}$$

where $N_{e\_cu}^{2d} \approx 1.9271 \times 10^{19}$ electrons/m^2 is the surface electron density and $m_e = 9.1 \times 10^{-31}$ kg is the mass of the electron and $v_{cu} = 41.667$ THz is the electron relaxation frequency of copper. Figure 1 shows a comparison between the dynamic conductivity of armchair carbon nanotubes for different values of m. It can be noted that the conductivity of the carbon nanotube decrease by increasing m. The imaginary part of the conductivity is zero at dc and it has a beak value around 50 GHz. The real part of the conductivity is decreasing by increasing the operating frequency.
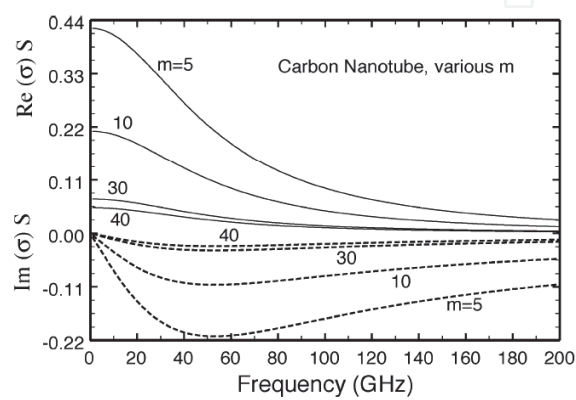
Fig. 1. Dynamic conductivity of armchair carbon nanotube for various m values. Solid lines are $\mathrm{Re}(\sigma)$; dashed lines are $\mathrm{Im}(\sigma)$. (Hanson 2005).
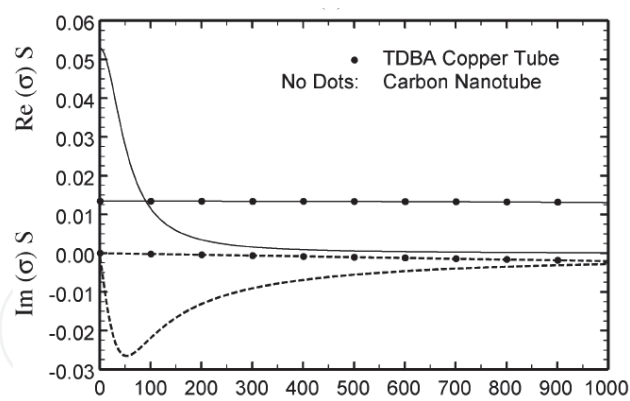

Fig. 2. Comparison between the conductivity of an armchair carbon nanotube of m = 40 and the conductivity of an infinitely thin copper tube of the same radius (2.712 nm) (Hanson 2005)

Figure 2 shows a comparison between the conductivity of an armchair carbon nanotube of m = 40 with the surface conductivity of a hollow copper tube of the same radius. It can be noted that the imaginary part of the copper conductivity is negligible from dc up to 1 THz. Below 100 GHz, the real part of the conductivity of carbon nanotube is greater the conductivity of copper. However, at higher frequencies both the real and imaginary parts of the conductivity saturate at much smaller values.

3. Electron fluid model of carbon nanotube transmission line

In this section electron fluid model is presented as an alternative representation to describe the linear response of a single wall metallic carbon nanotube to an applied electromagnetic field. This method is based on presenting the problem in the classical form of moving point charges in electric field with using appropriate effective mass for the moving electrons to include the effect of the carbon nanotube lattice. The nanotube is modeled as a continuous infinitesimally thin cylinder shell S of radius r_c and length l. The cylinder is oriented along the z-axis as shown in Figure 3. In thermodynamic equilibrium the π-electrons are distributed uniformly where the applied electromagnetic field perturbs this equilibrium distribution of the π-electrons.
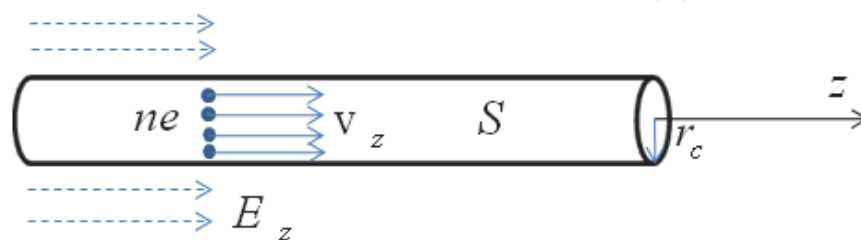

Fig. 3. Carbon nanotube geometry

The collective motion of the perturbed π-electrons is modeled by considering them as a charged fluid. Assuming that $v_z(\mathbf{r}_s, t)$ is the mean velocity of the electron fluid, where $\mathbf{r}_s$ is the position vector of an arbitrary point on the surface S; $n = n_0 + \delta n(\mathbf{r}_s; t)$ is the surface number density of the electron fluid, where n_0 is the equilibrium value; $p = p_0 + \delta p(\mathbf{r}_s; t)$ is the "two-dimensional" pressure of the electron fluid, where p_0 is the equilibrium value. The incremental pressure perturbation is related to the incremental electron density perturbation by the relation $\delta p = m_{eff} c_s^2 \delta n$ where c_s is the thermodynamic speed of sound of the electron fluid if it is neutral and m_{eff} is the mean effective mass of the π-electrons. This thermodynamic speed equals nearly electron Fermi velocity $c_s \approx v_F = 3\pi\gamma_0 b / h \approx 8 \times 10^5 m / s$ The motion of π-electron fluid follows the law of momentum conservation which can be presented in the present case as

$$n_0 m_{eff} \frac{\partial v_z}{\partial t} + v n_0 m_{eff} v_z + \frac{\partial \delta p}{\partial z} = n_0 e E_z \tag{13}$$

This momentum conservation equation can be presented in terms of the longitudinal current $I_z = 2\pi r_c e n v_z$ and the surface charge density $q = 2\pi r_c e n$ as follows

$$\frac{\partial I_z}{\partial t} + v I_z + c_s^2 \frac{\partial q}{\partial z} = \frac{2\pi r_c n_0 e^2}{m_{eff}} E_z \tag{14}$$

The parameter n_0 / m_{eff} takes into account the influence of the atomic crystal field. This parameter is obtained for the case of a conducting armchair carbon nanotube by using semiclassical model based on Boltzmann equation as $n_0 / m_{eff} \approx 4v_F / \pi h r_c$.

This representation corresponds to an equivalent distributed series RL per unit length with shunt quantum capacitance per unite length as shown in Figure 4, where

$$E_z = L_k \frac{\partial I_z}{\partial t} + R I_z + \frac{1}{C_q} \frac{\partial q}{\partial z} \qquad (15)$$

The elements of this equivalent circuit are the kinetic inductance per unit length $L_k = h / 8e^2 v_F$, the quantum capacitance per unit length $C_q = 8e^2 / hv_F$ and the ohmic resistance per unit length $R = vh / 8e^2 v_F$ respectively. Typical values of kinetic inductance and quantum capacitance are $L_K = 4\text{nH}/\mu\text{m}$ and $C_Q = 400a\text{F}/\mu\text{m}$ respectively.
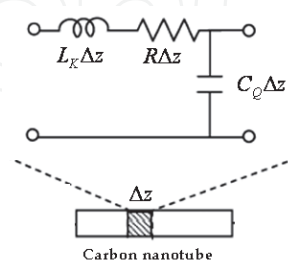

Fig. 4. Circuit model for electron flow along carbon nanotube

It is interesting to note that the series elements of this equivalent distributed circuit of carbon nanotube can be directly obtained by using the equivalent surface conductivity of armchair carbon nanotube which is discussed in the previous section as follows:

$$Z_s = \frac{1}{2\pi r_c \sigma_{zz}} = R + j\omega L_k \qquad (16)$$

However, the parallel quantum capacitance element cannot be obtained directly from this surface impedance since we neglected the longitudinal derivative of the electron distribution function in the derivation of the equivalent surface conductance. It would be shown in the following discussion that the wave propagation on carbon nanotube is mainly dominated by the kinetic inductance and the loss resistance. Thus, the approximation used in deriving surface conductance does not have a significant effect on studying electromagnetic wave propagation along carbon nanotube.

For the case of a carbon nanotube transmission line above a PEC ground plane as shown in Figure 5, the equivalent distributed circuit would be a combination of the equivalent circuit for electron current flow along the carbon nanotube and the conventional distributed transmission line circuit which is based on electrostatic capacitance and magnetostatic inductance of the transmission line structure. In the present case the distributed elements of the equivalent circuit of the transmission line per unit length are

$$L_M = (\mu_0 / 2\pi) \ln(2d / r_c) \qquad (17\text{-a})$$

$$C_E = 2\pi\varepsilon_0\varepsilon_r / \ln(2d / r_c) \qquad (17\text{-b})$$

where d is the separation distance between the carbon nanotube line and the ground plane and ε_r is the relative permittivity of the supporting substrate. A typical value of substrate thickness is between $100\,\overset{\circ}{\text{A}}$ and $1\,\mu m$ (Burke 2002) and Silicon dioxide substrate has a dielectric constant $\varepsilon_r = 4$. For a Silicon dioxide substrate of 0.2 μm thickness, typical values

of single wall carbon nanotube transmission line equivalent circuit parameters would be $C_{ES} \approx 50 aF/\mu m$, and $L_M \approx 1pH/\mu m$.
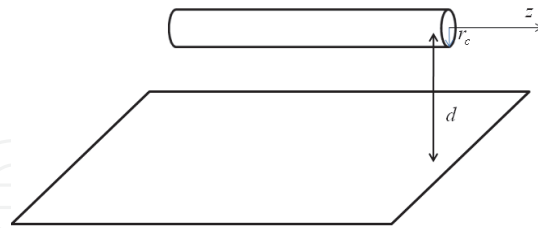

Fig. 5. Carbon nanotube transmission line above a PEC ground plane

In this case the effective inductance and resistance of the equivalent distributed circuit of the carbon nanotube transmission line above a ground plane are given by

$$L_{eff} = \left(L_M + L_k\right) / \left(1 + C_E / C_Q\right) \tag{18-a}$$

$$R_{eff} = R / \left(1 + C_E / C_Q\right) \tag{18-b}$$

while the effective capacitance in this case is the conventional electrostatic capacitance C_E. In addition to this equivalent distributed circuit, two additional contact resistances should be included at the two ends of the equivalent circuit of the carbon nanotube transmission line. The value of this contact resistance is given by $R_c = h / 8e^2$.

By comparing these values, it can be noted that the kinetic inductance is much larger than the magnetostatic inductance of transmission line section where the ratio of $L_k / L_M \approx 4 \times 10^3$. This means that the kinetic inductance has the dominant inductive effect on the equivalent distributed circuit. On the other hand, the quantum capacitance is nearly of the same order of the electrostatic capacitance of the transmission line section. This property has two main effects on electromagnetic wave propagation along the carbon nanotube transmission line; slow wave propagation and high characteristic impedance. The complex propagation constant, phase velocity and characteristic impedance in this case are given by:

$$\gamma = \alpha + j\beta = \sqrt{j\omega C_E \left(R_{eff} + j\omega L_{eff}\right)} \tag{19-a}$$

$$\lim_{R_{eff} \ll \omega L_{eff}} v_p = \lim_{R_{eff} \ll \omega L_{eff}} \frac{\omega}{\sqrt{\frac{1}{2}\left(\omega^2 C_E L_{eff} + \sqrt{\omega^4 C_E^2 L_{eff}^2 + \omega^2 C_E^2 R_{eff}^2}\right)}} \approx \sqrt{1 / L_{eff} C_E} \tag{19-2}$$

$$Z_c = \sqrt{\left(R_{eff} + j\omega L_{eff}\right) / j\omega C_E} \tag{19-c}$$

The phase velocity in this case is nearly of the same order of Fermi velocity v_F which is nearly two-order less than free space light speed. This means that the wavelength along carbon nanotube transmission line is nearly two-order less than conventional transmission

lines. This property has a significant importance in RF applications since the dimensions of passive circuits like filters, couplers and power dividers are comparable with operating wave length. However, these additional inductance and capacitance introduce high characteristic impedance of order 12.5 k Ω. Recently, parallel carbon nanotubes and carbon nanotube bundle have been introduced to overcome this disadvantage. The effective distributed elements of the equivalent circuit for a carbon nanotube bundle are simply the parallel combination of the circuit for a single carbon nanotube. Thus, both the effective inductance and resistance are divided by N and the effective quantum capacitance is multiplied by a factor N where N is the number of the nanotubes in the bundle. Different experimental results have shown that using parallel carbon nanotube decreases both the DC and RF impedance. However, it increases the wave velocity and subsequently the wave length. Thus, a compromise between the required wave velocity and characteristic impedance should be considered to select the appropriate number of carbon nanotubes in the bundle. On the other hand, the attenuation coefficient has a significant effect at the operating frequencies less than electron relaxation frequency where $\omega < R_{eff} / L_{eff} = \nu$. Thus at lower frequency band below relaxation frequency, carbon nanotube presents a good candidate for an absorbing structure more than a guiding structure.

4. Finite difference analysis of coupled Maxwell-Schrödinger equations

In this section we present another approach which is useful to study electromagnetic interaction with nanodevices like carbon nanotubes. This approach is based on coupling Schrödinger equation which describes the motion of charged particles along the nanodevice with Maxwell's equations which describe the electromagnetic waves in the region of the nanodevice. Both Schrödinger and Maxwell's equations can be presented as partial differential equations which can be solved numerically by using finite difference scheme based on specific sources and boundary conditions. This approach is quite useful to study electromagnetic field interaction with short nanotubes of length less than 100 nm where the electron transport is nearly ballistic.

The quantum motion of electrons along a nanodevice can be presented by Schrödinger equation as follows:

$$j\frac{h}{2\pi}\frac{\partial \psi(\mathbf{r},t)}{\partial t} = \left(-\frac{h^2}{8\pi^2 m}\nabla^2 + V(\mathbf{r})\right)\psi(\mathbf{r},t) \tag{20}$$

where $\psi(\mathbf{r},t)$ is the complex state variable of the electron on the nanodevice and $V(\mathbf{r})$ is the static potential along this nanodevice. The key difference between different nanodevices lies in this static potential. In the presence of time-varying electromagnetic fields, Schrödinger equation is modified as follows:

$$j\frac{h}{2\pi}\frac{\partial \psi(\mathbf{r},t)}{\partial t} = \frac{1}{2m}\left(-\frac{h^2}{4\pi^2}\nabla^2\psi(\mathbf{r},t) - j\frac{he}{2\pi}\nabla \cdot \left(\mathbf{A}(\mathbf{r},t)\psi(\mathbf{r},t)\right)\right.$$
$$\left. - j\frac{he}{2\pi}\mathbf{A}(\mathbf{r},t)\cdot\nabla\psi(\mathbf{r},t) + e^2\,|\,\mathbf{A}(\mathbf{r},t)|^2\,\psi(\mathbf{r},t)\right) \tag{21}$$
$$ + \left(e\phi(\mathbf{r},t)\psi(\mathbf{r},t) + V(\mathbf{r})\psi(\mathbf{r},t)\right)$$

where $\mathbf{A}(\mathbf{r},t)$ is the applied magnetic vector potential, $\phi(\mathbf{r},t)$ is the applied scalar electric potential and e here represents the absolute value of the electron charge. The resulting quantum current density along the nanodevice can be presented in terms of this electron state variable as follows:

$$\mathbf{J}(\mathbf{r},t) = \frac{e^2}{m} |\psi(\mathbf{r},t)|^2 \, \mathbf{A} - j\frac{he}{4\pi m}\left(\psi*(\mathbf{r},t)\nabla\psi(\mathbf{r},t) - \psi(\mathbf{r},t)\nabla\psi^*(\mathbf{r},t)\right) \tag{22}$$

On the other hand, electromagnetic fields are related by Maxwell's equations as follows:

$$\nabla \times \mathbf{H}(\mathbf{r},t) = \varepsilon\frac{\partial \mathbf{E}(\mathbf{r},t)}{\partial t} + \mathbf{J}(\mathbf{r},t) \tag{23-a}$$

$$\nabla \times \mathbf{E}(\mathbf{r},t) = -\mu\frac{\partial \mathbf{H}(\mathbf{r},t)}{\partial t} \tag{23-b}$$

where the electric and magnetic field components can be presented in terms of the scalar electric potential and vector magnetic potential as:

$$\mathbf{E}(\mathbf{r},t) = -\nabla\phi(\mathbf{r},t) - \frac{\partial \mathbf{A}(\mathbf{r},t)}{\partial t} \tag{24-a}$$

$$\mathbf{H}(\mathbf{r},t) = \frac{1}{\mu}\nabla \times \mathbf{A}(\mathbf{r},t) \tag{24-b}$$

The scalar electric potential and the magnetic vector potential are related by Lorentz condition:

$$\frac{\partial\phi(\mathbf{r},t)}{\partial t} = -\frac{1}{\mu\varepsilon}\nabla \cdot \mathbf{A}(\mathbf{r},t) \tag{25-a}$$

and the magnetic vector potential is related to the current density by non-homogenous wave equation:

$$\frac{\partial^2 \mathbf{A}(\mathbf{r},t)}{\partial t^2} = \frac{1}{\mu\varepsilon}\nabla^2\mathbf{A}(\mathbf{r},t) - \frac{1}{\varepsilon}\mathbf{J}(\mathbf{r},t) \tag{25-b}$$

By solving Equations (21)-(25), one can obtain electromagnetic interaction with the proposed nanodevice. Numerical solution of these coupled partial differential equations can be obtained by using finite difference method. This method is based on approximating the differential operator by a difference operator to obtain the required quantities on the nodes of a discrete mesh in the space $(i\Delta x, j\Delta y, k\Delta z)$ at discrete steps in time $(n\Delta t)$. To simplify the problem, the complex state variable of Equation (21) is divided into real and imaginary parts as follows:

$$\psi(\mathbf{r},t) = \psi_R(\mathbf{r},t) + j\psi_I(\mathbf{r},t) \tag{26}$$

Thus, Equation (21) can be reformulated as two coupled partial differential equations of pure real variables:

$$\frac{\partial \psi_R(\mathbf{r},t)}{\partial t} = \frac{1}{2m}\Bigg(-\frac{h}{2\pi}\nabla^2 \psi_I(\mathbf{r},t) - e\nabla \cdot \mathbf{A}(\mathbf{r},t)\psi_R(\mathbf{r},t)$$

$$-2e\mathbf{A}(\mathbf{r},t)\cdot\nabla\psi_R(\mathbf{r},t) + \frac{2\pi}{h}e^2\,|\,\mathbf{A}(\mathbf{r},t)\,|^2\,\psi_I(\mathbf{r},t)\Bigg) \qquad (27\text{-}a)$$

$$+\Bigg(\frac{2\pi}{h}e\phi(\mathbf{r},t)\psi_I(\mathbf{r},t) + \frac{2\pi}{h}V(\mathbf{r})\psi_I(\mathbf{r},t)\Bigg)$$

$$\frac{\partial \psi_I(\mathbf{r},t)}{\partial t} = \frac{1}{2m}\Bigg(\frac{h}{2\pi}\nabla^2 \psi_R(\mathbf{r},t) - e\nabla \cdot \mathbf{A}(\mathbf{r},t)\psi_I(\mathbf{r},t)$$

$$-2e\mathbf{A}(\mathbf{r},t)\cdot\nabla\psi_I(\mathbf{r},t) - \frac{2\pi}{h}e^2\,|\,\mathbf{A}(\mathbf{r},t)\,|^2\,\psi_R(\mathbf{r},t)\Bigg) \qquad (27\text{-}b)$$

$$-\Bigg(\frac{2\pi}{h}e\phi(\mathbf{r},t)\psi_R(\mathbf{r},t) + \frac{2\pi}{h}V(\mathbf{r})\psi_R(\mathbf{r},t)\Bigg)$$

For the case of a carbon nanotube where the length of the nanotube is usually much larger than its diameter, the problem can be presented as 1-D problem along the length of the nanotube. In this case the ∇ operator in the above equation can be simply replaced by $\partial / \partial z\, \mathbf{a}_z$.

The scalar electric potential and magnetic vector potentials are assumed to be known at the time steps n and $n+1/2$. Thus by discretizing Equation (25-b) one can obtain the update equation of the magnetic vector potential at time step $n+1$ as follows:

$$A_z^{n+1}(k) = 2A_z^{n+1/2}(k) - A_z^n(k)$$

$$+\frac{(\Delta t/2)^2}{\mu\varepsilon(\Delta z)^2}\Big(A_z^{n+1/2}(k+1) - 2A_z^{n+1/2}(k) + A_z^{n+1/2}(k-1)\Big) - \frac{(\Delta t/2)^2}{\varepsilon}J_z^{n+1/2}(k) \qquad (28)$$

Based on the result of Equation (28) and the previously stored electric potential and vector potentials, one can obtain the update equation for the electric field along the nanotube at the time step $n+1/2$ by discretizing Equation (24-a)

$$E_z^{n+1/2}(k) = -\frac{\phi^{n+1/2}(k+1) - \phi^{n+1/2}(k-1)}{2\Delta z} - \frac{A_z^{n+1}(k) - A_z^n(k)}{\Delta t} \qquad (29)$$

The update equations of the electric fields at the time step $n + 1/2$ in the remaining domain outside the nanotube can be obtained by using conventional FDTD formulation for the differential form of Ampere's law, Equation (23-a),

$$\mathbf{E}^{n+1/2}(\mathbf{r},t) = \mathbf{E}^{n-1/2}(\mathbf{r},t) + \frac{\Delta t}{\varepsilon}\nabla\times\mathbf{H}^n(\mathbf{r},t) \qquad (30)$$

It should be noted that we assumed here the present current density is limited to the nanotube structure only which is already included in Equation (29). Thus Equation (30) does not include an electric current term. Similarly, the update equations of the magnetic fields at the time step $n + 1$ are obtained by using conventional FDTD formulation for the differential form of Faraday's law, Equation (23-b),

$$\mathbf{H}^{n+1}(\mathbf{r},t) = \mathbf{H}^n(\mathbf{r},t) - \frac{\Delta t}{\mu}\nabla\times\mathbf{E}^{n+1/2}(\mathbf{r},t) \tag{31}$$

The update equations of the scalar electric potential function at the time step n+1 can be obtained by discretizing Equation (25-a) as follows:

$$\phi^{n+1}(k) = \phi^n(k) - \frac{1}{\mu\varepsilon}\frac{\Delta t}{2\Delta z}\left(A_z^{n+1/2}(k+1) - A_z^{n+1/2}(k-1)\right) \tag{32}$$

To obtain the above quantities at the following time step, it is required to update the potential functions and the current density to the time step n+3/2. To do this it is required to use Schrödinger equation to update the state variable and consequently the current density and the potential functions. Assuming that the state variables are known at time steps n and n+1/2, one can obtain the temporal update equation of the real and imaginary parts of the complex state function at the time step n+1 in the following forms:

$$\begin{aligned}
\psi_R^{n+1}(k) = \psi_R^n(k) &- \frac{h\Delta t}{4m\pi}\frac{\psi_I^{n+1/2}(k+1) - 2\psi_I^{n+1/2}(k) + \psi_I^{n+1/2}(k-1)}{(\Delta z)^2} \\
&- \frac{e\Delta t}{2m}\frac{A_z^{n+1/2}(k+1) - A_z^{n+1/2}(k-1)}{2\Delta z}\psi_R^{n+1/2}(k) \\
&- \frac{e\Delta t}{m}A_z^{n+1/2}(k)\frac{\psi_R^{n+1/2}(k+1) - \psi_R^{n+1/2}(k-1)}{2\Delta z} + \frac{\pi\Delta t}{mh}e^2\left(A_z^{n+1/2}(k)\right)^2\psi_I^{n+1/2}(k) \\
&+ \left(\frac{2\pi\Delta t}{h}e\phi^{n+1/2}(k)\psi_I^{n+1/2}(k) + \frac{2\pi\Delta t}{h}V(k)\psi_I^{n+1/2}(k)\right)
\end{aligned} \tag{33-a}$$

$$\begin{aligned}
\psi_I^{n+1}(k) = \psi_I^n(k) &+ \frac{h\Delta t}{4m\pi}\frac{\psi_R^{n+1/2}(k+1) - 2\psi_R^{n+1/2}(k) + \psi_R^{n+1/2}(k-1)}{(\Delta z)^2} \\
&- \frac{e\Delta t}{2m}\frac{A_z^{n+1/2}(k+1) - A_z^{n+1/2}(k-1)}{2\Delta z}\psi_I^{n+1/2}(k) \\
&- \frac{e\Delta t}{m}A_z^{n+1/2}(k)\frac{\psi_I^{n+1/2}(k+1) - \psi_I^{n+1/2}(k-1)}{2\Delta z} - \frac{\pi\Delta t}{mh}e^2\left(A_z^{n+1/2}(k)\right)^2\psi_R^{n+1/2}(k) \\
&- \left(\frac{2\pi\Delta t}{h}e\phi^{n+1/2}(k)\psi_R^{n+1/2}(k) + \frac{2\pi\Delta t}{h}V(k)\psi_R^{n+1/2}(k)\right)
\end{aligned} \tag{33-b}$$

Based on this complex state variable, one can obtain the current density at the time step n+1 by discretizing Equation (22) as follows:

$$\begin{aligned}
J_z^{n+1}(k) = \frac{e^2}{m}&\left(\left[\psi_R^{n+1}(k)\right]^2 + \left[\psi_I^{n+1}(k)\right]^2\right)A_z^{n+1} - \frac{he}{2\pi m}\left(\psi_I^{n+1}(k)\frac{\psi_R^{n+1}(k+1) - \psi_R^{n+1}(k-1)}{2\Delta z}\right) \\
&+ \frac{he}{2\pi m}\left(\psi_R^{n+1}(k)\frac{\psi_I^{n+1}(k+1) - \psi_I^{n+1}(k-1)}{2\Delta z}\right)
\end{aligned} \tag{34}$$

At this point we have $\phi^{n+1}(k)$, $A_z^{n+1}(k)$, $\psi_R^{n+1}(k)$, $\psi_I^{n+1}(k)$ and $J_z^{n+1}(k)$ in addition to the previously calculated quantities. By repeating the same steps from Equations (32) to (34) and

Equation (28), one can obtain state parameters, current density and potential functions at $n+3/2$ time step. Thus we obtain scalar electric potential and magnetic vector potentials at the time steps $n+1$ and $n+3/2$. Then by repeating the same steps of Equations (28) to (31) one can obtain the electric and magnetic fields in the following time step.

The above analysis represents the core of the finite difference time domain formulation of the coupled Maxwell-Schrödinger equations for solving electromagnetic coupling with nanodevice with emphasis on simple linear nanodevices like carbon nanotube. It should be noted that there are many other problems in this method which require more investigation like absorbing boundary conditions for Schrödinger equation, stability and dispersion. (Pierantoni *et al.*; 2008, Pierantoni *et al.*; 2008 & Ahmed *et al.* 2010)

5. Surface wave propagation along carbon nanotubes

Carbon nanotubes can also be considered as cylindrical guiding structures of finite conductivity. This section shows how to determine the complex propagation constant of this guiding structure based on its macroscopic conducting properties. Since we are mainly concerned with the longitudinal conductivity, the propagating wave along the nanotube would be mainly TM wave. In this case the total field can be represented in terms of the axial TM Hetezian potential Π_e as follows:

$$\vec{E} = \nabla\left(\nabla \cdot \Pi_e\right) + k_0^2 \Pi_e \tag{35-a}$$

$$\vec{H} = j\omega\varepsilon_o \nabla \times \Pi_e \tag{35-b}$$

where the TM Hertezian potential is determined by solving the wave equation

$$\nabla^2 \Pi_e + k_0^2 \Pi_e = 0 \tag{36}$$

For a cylindrical configuration, the general solution of wave equation can be presented as Bessel functions. The field inside the cylinder is finite in the range $0 \leq \rho \leq r$ where r is the radius of the proposed cylinder. Thus the field in this region is represented by Bessel function of first kind. On the other hand, the field outside the cylinder is finite at $\rho = r$ and is exponentially decaying for $\rho = r$. Thus, the field in this region is represented by Hankel function of second kind. Hence, the general solution of the TM Hertizian potential in carbon nanotube (single or a circular bundle) can be represented as:

$$\Pi_e = A\vec{a}_z \begin{Bmatrix} \mathrm{J}_n(\kappa\rho)\mathrm{H}_n^{(2)}(\kappa r) \\ \mathrm{J}_n(\kappa r)\mathrm{H}_n^{(2)}(\kappa\rho) \end{Bmatrix} e^{-j\gamma z}e^{-jn\varphi} \quad \begin{matrix} \rho \leq r \\ \rho \geq r \end{matrix} \tag{37}$$

By using this Hertezian potential in Equation (35) and applying the boundary condition

$$J_z = \sigma_{zz}E_z(r) = -\lim_{\delta \to 0}\left[H_\phi(r+\delta) - H_\phi(r-\delta)\right] \tag{38}$$

one can obtain the dispersion equation for surface wave propagation as follows:

$$\left(\frac{\kappa}{k_0}\right)^2 J_n(\kappa r) H_n^{(2)}(\kappa r) = \frac{2}{\pi \sigma_{zz} Z_0 k_0 r} \quad \text{where} \ \operatorname{Im}(\kappa) \le 0 \tag{39}$$

The longitudinal propagation constant is given by:

$$\gamma = \sqrt{k_0^2 - \kappa^2} \quad \text{where} \ \operatorname{Im}(\gamma) \le 0 \tag{40}$$

It would be useful here to study the limit of the above dispersion equation for the zero-order mode at small argument limit. In this case the Bessel function combination of the right hand side can be approximated as:

$$J_0(\kappa r) H_0^{(2)}(\kappa r) \approx \left(1 - j\frac{2}{\pi}\Big[\ln(\kappa r/2) + 0.577215)\Big]\right) \tag{41}$$

Unlike Bessel function, the logarithmic function in the right hand side of Equation (41) can be represented by a slowly convergent series for small argument. However, for gigahertz frequency band, the average value of this logarithmic function is nearly around minus ten. Thus, an approximate value of the zero order mode complex surface wave propagation coefficient along a carbon nanotube is given by:

$$\gamma \approx k_0 \sqrt{1 - \frac{1}{\sigma_{zz} Z_0 k_0 r (\pi/2 + j10)}} \tag{42}$$

It can be noted that, by increasing the longitudinal conductivity of the tube the surface wave propagation constant approaches the free space propagation constant.
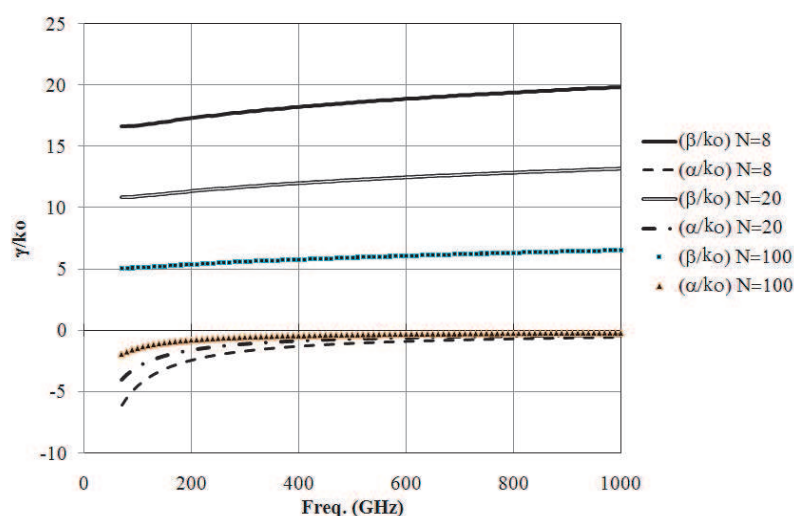

Fig. 6. Surface wave propagation on carbon nanotube bundles of different values of *N*. The bundle is composed of armchair carbon nanotubes with lattice parameters $m = n = 40$. (Attiya 2009)

Figure 6 shows complex wave propagation constant of TM surface waves along a carbon nanotube circular bundle for different values of *N* where *N* is the number of carbon nanotubes in the bundle. The present results are based on armchair carbon nanotubes of $m = n = 40$. For

this configuration, the radius of the nanotube is r_c = 2.7nm. For a closely backed bundle composed of N carbon nanotubes arranged in a single circular shell the radius of the bundle is

$$r = 2Nr_c / \pi \qquad (43\text{-}a)$$

In this case the effective axial surface conductivity of this shell can be approximated by

$$\sigma_{zz}^b \approx N\sigma_{zz}^{cn} r_c / r \qquad (43\text{-}b)$$

It can be noted that the attenuation coefficient increases by decreasing the operating frequency as shown in Figure 6. The effect of this attenuation coefficient is negligible in the frequency range from 100 to 1000 GHz. On the other hand, this attenuation coefficient has a significant effect in the frequency band below 100 GHz.

6. Carbon nanotube antenna

Carbon nanotube can also be a good candidate for antenna structures. Slow wave property of electromagnetic propagation along carbon nanotube is expected to play an important role in reducing the size of resonant carbon nanotube antenna. From the mathematical point of view, carbon nanotube antennas can be treated as an antenna composed of finite-conducting cylinders. In this case the dynamic conductivity derived in Section 2 is used to include the electrical properties of carbon nanotube in the mathematical modeling of the corresponding antenna structure. This electromagnetic formulation can be presented in any form like integral equation, finite difference or finite element. However, for simple wire antenna configuration, electric field integral equation method may be the most appropriate method. Thus we would focus on this method in the following part of this section.

For the case of a simple dipole antenna oriented along the z axis, the relation between the excitation field and the current distribution can be presented by Hallen's integral equation as follows:

$$\int_{-L}^{L} \left(\frac{e^{-jk_0\sqrt{(z-z')^2+r^2}}}{\sqrt{(z-z')^2+r^2}} + \frac{1}{Z_0\sigma_{zz}r}e^{-jk_o|z-z'|} \right) I(z')dz' = C\cos k_0 z - j\frac{4\pi\omega\varepsilon_0}{2k_0}\sin k_0 |z-z_0| \qquad (44)$$

where r is the radius of the dipole ($r = r_c$ for single nanotube) and σ_{zz} is the effective surface conductivity of the dipole, z_0 is the location of the feeding point, C is a constant that would be determined to satisfy the current vanishing at the edges of the dipole and L is the half length of the dipole. The effect of the carbon nanotube in this integral equation lies in surface conductivity and the radius of the nanotube. This formulation can be used to simulate a dipole antenna composed of single carbon nanotube or a bundle of carbon nanotubes. In the case of a carbon nanotube bundle, the corresponding radius and surface conductivity are obtained by Equation (43).

This integral equation can be solved numerically by using method of moments to find out the current distribution and subsequently the input impedance, radiation pattern, radiation efficiency and other antenna parameters. This method is based on expanding the unknown current distribution as a finite series of known basis functions of unknown amplitudes. To determine these amplitudes, Equation (44) is weighted by a set of weighting functions

which equals the number of the unknown amplitudes. Thus, Equation (44) is converted into a system of equations which is solved to obtain the unknown amplitudes of the current distribution functions. Details of solving this integral equation numerically by using method of moments can be found in (Elliot 2003).

Figure 7 shows the complex input impedance of a dipole of a carbon nanotube for two cases as functions of the operating frequency. The present results are based on conducting armchair carbon nanotubes of $m = n = 40$. The length of the dipole is assumed to be 30 μm and 1 mm for the first and second case respectively. It can be noted that the first case has a first resonance at nearly 160 GHz. However, the second case does not have any resonance. Figure 8-a shows the current distribution along the 10 μm dipole antenna at its first resonance frequency due to a unity voltage source at its feeding point. It can be quite clear that the dipole in this case corresponds to a half-guided-wave length dipole. It can also be noted that the length of the first resonant carbon nanotube antenna is nearly 0.0107 times the length of conventional half-wave length dipole at this frequency. This represents an important feature of carbon nanotube antenna. It can also be noted the corresponding input impedance in this case is nearly 11 kΩ which is much greater than the conventional input impedance of a half-wave dipole which is nearly of order 75Ω. On the other hand, the current distribution along the 1 mm dipole antenna has different properties as shown in Figure 8-b, where the real and imaginary parts of the current are concentrated around the center of the dipole and highly damped at its ends. It can be concluded from this result that the problem of carbon nanotube antenna at different frequency ranges cannot be directly obtained by simple scaling as the case in perfect electric conductor.

Figure 9 shows the input impedance of a dipole of a carbon nanotube bundle for different values of N. The length of the dipole is taken to be 30 μm and 3000 μm. It can be noted that the 30 μm dipole has a first resonance, that corresponds to a half-guided-wave length dipole for N = 8, at 280 GHz. The resonance impedance in this case is nearly 2100 Ohms. By

(a) The length of the dipole is 10 μm (b) The length of the dipole is 1 mm

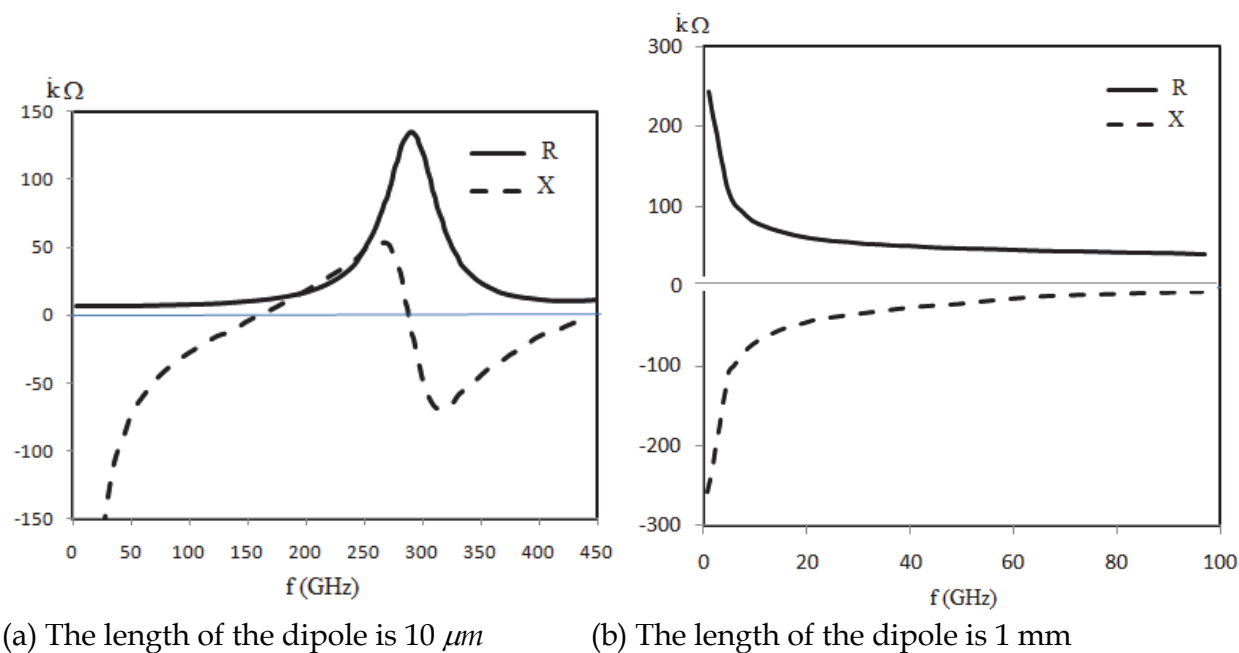Fig. 7. Input impedance for a carbon nanotube antenna. The carbon nanotube is armchair of lattice parameters m=n=40.

comparing this length with free space half-wave at this frequency it can be noted that this carbon nanotube antenna has a reduction scale factor of nearly 0.056 compared with conventional half-wave length dipole. Increasing the number of nanotubes in the bundle decreases the total surface impedance of the dipole. This has two effects, increasing the resonance frequency for a specific length and decreasing the resonance impedance as shown in the case where N is increased to twenty. In this case the first resonance frequency is 404 GHz and the resonance impedance is 840 Ohms. The scale reduction factor in this case is nearly 0.081. For a hundred nanotube bundle of the same length, the resonance frequency would be 740 GHz and the resonance impedance would be 174 Ohms. In this case the scale reduction factor is nearly 0.15. It can be noted that by increasing the number of carbon nanotubes in the bundle, both resonance frequency and reduction factor are increased while the input impedance is decreased. On the other hand, the 3000 μm dipole does not introduce resonance behavior for any value of N as it is shown in Figure 9-b. This result is quite similar to the results of a single carbon nanotube antenna shown in Figure 7.
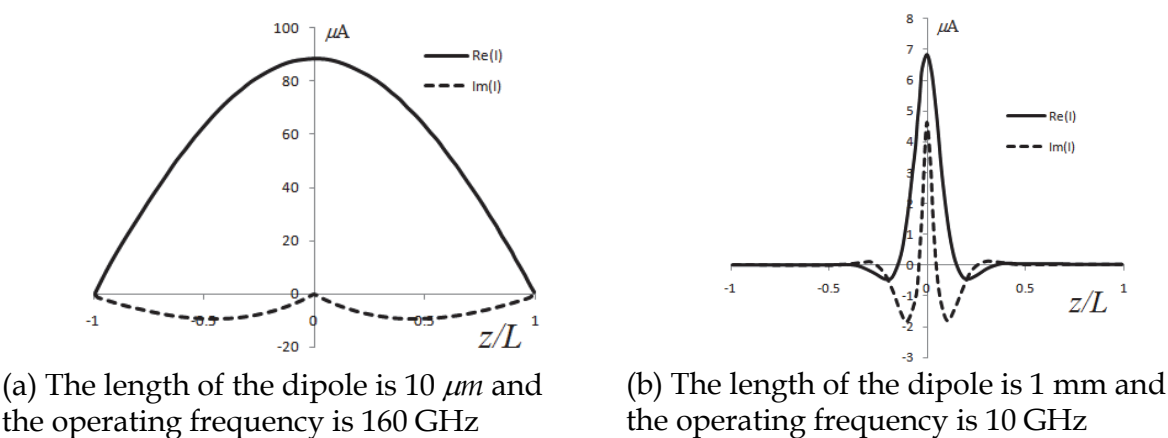

(a) The length of the dipole is 10 μm and the operating frequency is 160 GHz

(b) The length of the dipole is 1 mm and the operating frequency is 10 GHz

Fig. 8. Current distributions along carbon nanotube dipole antennas due to a unity voltage source.

(a) L = 30 μm

(b) L = 3000 μm
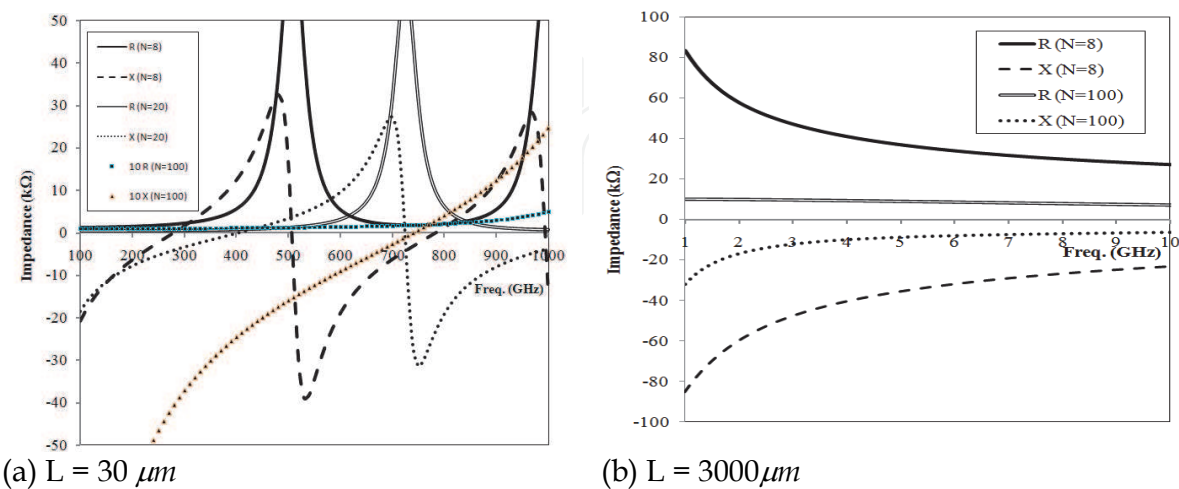
Fig. 9. Input impedance of bundle dipole. The bundle is composed of armchair carbon nanotubes with lattice parameters $m = n = 40$. Numbers of nanotubes in the bundles are N=8, N=20 and N=100 (Attiya 2009)

It is noted that the inverse reduction factors of the resonant bundle dipoles equals nearly the ratio of the surface wave propagation constant with respect to the free space wave number shown in Figure 6 for the same bundles. These results show the relation between the resonant dipole length and the surface wave velocity on its arms. On the other hand, by studying the surface wave complex wave propagation constant, it can be noted that the attenuation coefficient increases by decreasing the operating frequency as shown in Figure 6. The effect of this attenuation coefficient is negligible in the frequency range from 100 to 1000 GHz. Thus, the main behavior of the input impedance of the dipole antenna is nearly the same of traditional dipole antenna with taking into account scaling reduction factor due to the slow surface wave velocity. However, in the band from 1 to 10 GHz, the wave propagating on the arms of the dipole is attenuated. Thus, the reflected wave does not add completely at the feeding point which means the inductive effect due to the delayed reflected signal does not compensate completely the capacitive effect of the dipole arms. This explains the capacitive behavior of CNT dipoles in Figures 7-b and 9-b. In this case, the wave propagating on the arms of the dipole is highly attenuated, such that the active part of the dipole is much smaller than the physical length of the dipole itself. Thus, the dipole would always be a short dipole in this case and it is not resonant in any case. This result shows that the advantage of size reduction combined with surface wave propagation can be used only in high frequency bands above 100 GHz.

7. Carbon nanotubes in passive RF circuits

Recent advances in carbon nanotubes make them competitive elements in many RF applications. New fabrication techniques can be used to synthesize and electrically contact single carbon nanotube up to nearly 1 cm (Li *et al.* 2007). In addition using solubilized carbon nanotube and dielectrophoresis can be used to accumulate hundreds to thousands of carbon nanotubes in parallel (Rutherglen *et* al. 2008). These advances in fabrication techniques open the door for more research on different configurations of carbon nanotubes which are believed to be visible in near future.

On the other hand, metallic single-wall carbon nanotube transmission line shows an important advantage of slow electromagnetic wave propagation compared with free space wave velocity. This wave velocity reduction is due to the additional kinetic inductance and quantum capacitance in the equivalent circuit model of the nanotube transmission line circuit. In this case the wave velocity along the single-wall carbon nanotube transmission line has the same order of Fermi velocity which is nearly 8×10^5 m/s. This means that the wave velocity in this case is nearly two-order less than free space wave velocity. Thus the wavelength along the single-wall carbon nanotube transmission line is nearly two-order smaller than free space wave length. This property is quite useful to reduce the physical dimensions of microwave circuits to be in hundred-micrometer scale instead of centimeter scale. However, these additional inductance and capacitance introduce high characteristic impedance of order 12.5 k Ω. In addition, the single-wall carbon nanotube transmission line has an intrinsic resistance of 6.5 kΩ and Ohmic contact resistance of order 20 kΩ which introduce high attenuation coefficient. These parameters make carbon nanotube transmission line is not suitable for microwave applications from the point of view of characteristic impedance and attenuation.

Recently, parallel carbon nanotube and carbon nanotube bundle have been introduced to overcome these disadvantage (Attiya & Kanhal, 2009). Different experiments introduced by

different authors have shown that using parallel carbon nanotube decreases both the DC and RF impedance; for example a bundle composed of ten parallel single wall carbon nanotube shows a DC impedance around 750Ω while hundreds of parallel single wall carbon nanotubes show an AC impedance from 60 to 40Ω in the frequency range from few MHz to 20 GHz (Rutherglen *et al.* 2008). These experimental results introduced the possibility of using parallel single wall carbon nanotubes to obtain nearly matched transmission line sections with low wave velocity. Parallel carbon nanotube transmission line sections can be used to replace traditional printed transmission line sections in microwave circuits to have a significant reduction in the total size of these circuits. However, one should consider the lossy and mismatch effects of parallel carbon nanotube transmission line. Further theoretical and experimental investigations are still required to study the possibility of using parallel carbon nanotube transmission lines in passive microwave circuits like hybrid couples, power dividers, filters… etc.

Other RF and microwave applications like switches, filters and resonators can also be obtained by using electromechanical propertied of carbon nanotubes. (Demoustier *et al.* 2008) introduced an RF nanoswitch based on vertically aligned carbon nanotubes. It consists of carbon nanotube perpendicular to the substrate. Two different architectures are proposed for this carbon nanotube switch; series-based switch using ohmic contact between carbon nanotubes and a capacitive-based switch implemented in shunt configuration. RF ohmic switch is designed by implementing carbon nanotubes in two sides of a coplanar waveguide discontinuity as shown on Figure 10-a. By applying dc voltage on the two sides of the coplanar waveguide discontinuity, an electrostatic force is introduced between the two arms of the carbon nanotube switch. This electrostatic closes the switch and the RF signal is transmitted across the coplanar waveguide as shown in Figure 10-b. On the other hand, shunt switch is based on two nanotube capacitive contacts between the inner line and the two sides of the ground planes of the coplanar waveguide as shown in Figure 11-a. By applying dc voltage between the inner and outer sides of the coplanar waveguide, the electrostatic field introduces a short circuit between the inner and the outer sides as shown in Figure 11-b. This short circuit reflects the propagating wave along the coplanar waveguide which corresponds to switching off the RF signal. To achieve the expected performance in the required operating frequency band, two inductive sections are added along the coplanar waveguide in series with nanotube to perform a series LC resonance at the center of operating frequency band. This resonant LC circuit introduces higher isolation level in the switch isolation state.
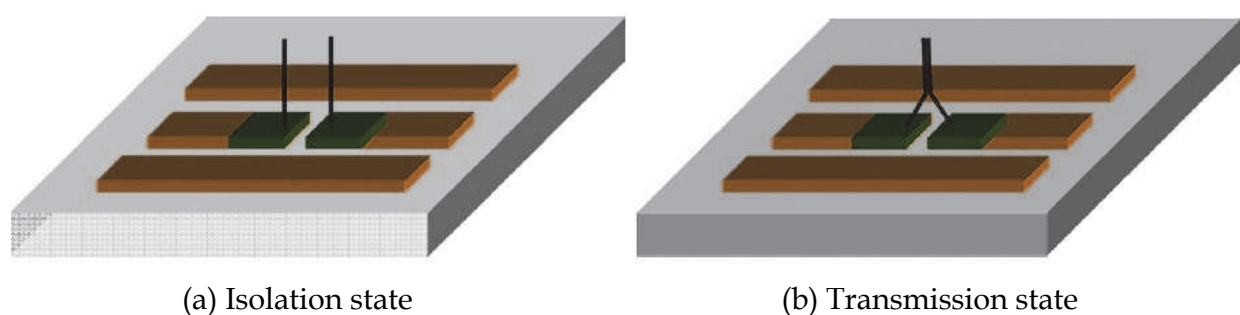

(a) Isolation state   (b) Transmission state

Fig. 10. Architecture of Carbon nanotube ohmic switch (Demoustier 2008)

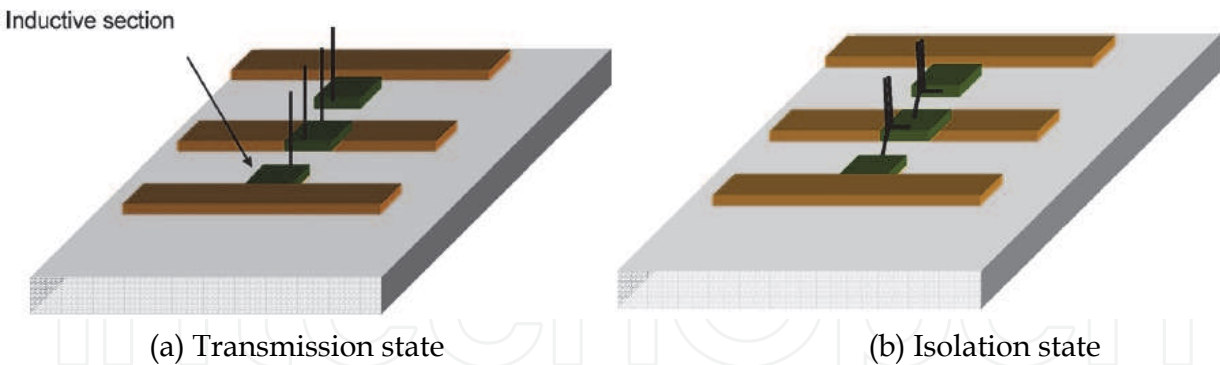(a) Transmission state   (b) Isolation state

Fig. 11. Architecture of Carbon nanotube shunt capacitive switch (Demoustier 2008)

Another application for carbon nanotubes in passive RF circuits based on their electromechanical properties is the microwave resonator and filter (Dragoman 2005). It is found that carbon nanotube has a mechanical resonance in the frequency range from 1 to 3 GHz with quality factor of 1000. The basic theory of carbon nanotube filter is based on coupling the electromagnetic fields of the incident signal to a perpendicular array of carbon nanotubes. This can be obtained by inserting this array of carbon nanotubes inside a coplanar waveguide as shown in Figure 13. In this case the coplanar waveguide transmits only the signals which are resonant with carbon nanotube array. To introduce the coupling between the incident electromagnetic wave and the carbon nanotube array, it is required to produce electric charges on the carbon nanotube. These electric charges are obtained by applying a dc electric field parallel to the direction of electromagnetic wave propagation and orthogonal on carbon nanotubes as shown in Figure 13. The presence of these electric charges introduces Coulomb forces between the carbon nanotubes and the electric field of the incident wave. The resonance of this filter is controlled by the value of the applied dc voltage. The vibration of the excited tubes located near the input electrode is propagating along the entire array like an acoustic excitation.
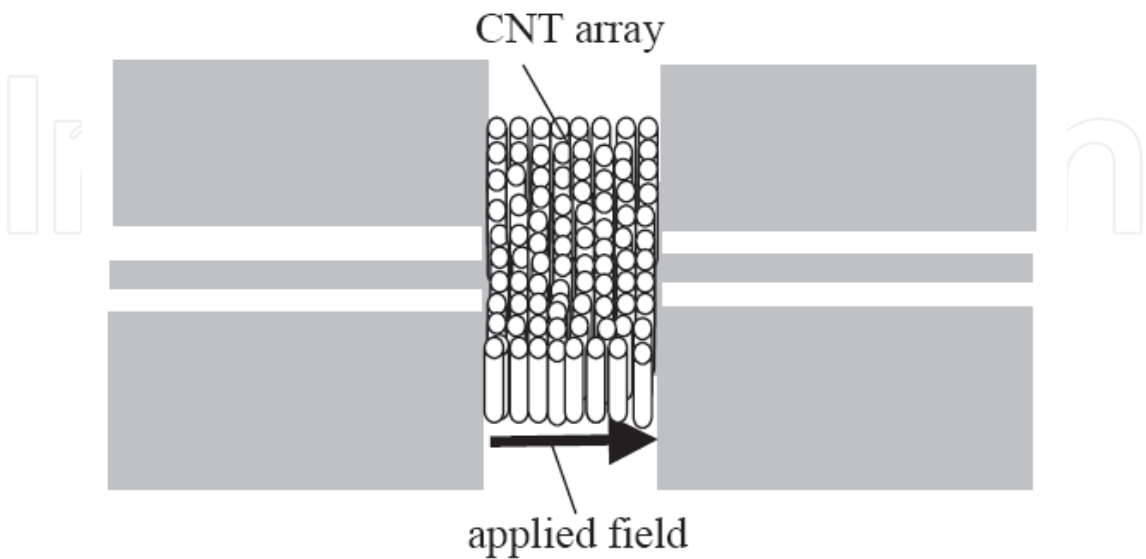

Fig. 13. Architecture of an RF bandpass filter based on a carbon nanotube array.

8. Carbon nanotubes composites for RF absorbing and shielding applications

From the above discussions about the possibility of using carbon nanotubes in microwave circuits it can be concluded that the high attenuation coefficient of wave propagation along carbon nanotube represents a main limiting factor in these application which may be overcome by using bundle of carbon nanotubes. However, this attenuation property is quite important in other microwave applications like absorbing and shielding. For these applications it is not required to arrange the carbon nanotubes in a bundle like the cases of antennas, transmission lines and interconnects. However, carbon nanotubes in these cases are mixed with other materials in a random form.

The effective dielectric constant of a dielectric mixture including conducting particles can be formulated by using Maxwell-Granett mixing rule as follows (Koledintseva 2009):

$$\varepsilon_{eff} = \varepsilon_b + \frac{\frac{1}{3}f_i\left(\varepsilon_i - \varepsilon_b\right)\sum_{k=1}^{3}\frac{\varepsilon_b}{\varepsilon_b + N_{ik}\left(\varepsilon_i - \varepsilon_b\right)}}{1 - \frac{1}{3}f_i\left(\varepsilon_i - \varepsilon_b\right)\sum_{k=1}^{3}\frac{N_{ik}}{\varepsilon_b + N_{ik}\left(\varepsilon_i - \varepsilon_b\right)}} \tag{45}$$

where ε_b is the relative permittivity of the base dielectric, ε_i is the permittivity of the inclusion particles, f_i is the volume fraction occupied by the inclusion, N_{ik} is the depolarization factor of the inclusions and the index $k = 1,2,3$ corresponds to x,y and z in Cartesian coordinates. The depolarization factors for an ellipsoid inclusion of radii a,b and c in x,y and z directions are given by:

$$N_{i1} = \frac{abc}{2}\int_{0}^{\infty}\frac{1}{(s+a)\sqrt{(s+a)(s+b)(s+c)}}ds \tag{46-a}$$

$$N_{i2} = \frac{abc}{2}\int_{0}^{\infty}\frac{1}{(s+b)\sqrt{(s+a)(s+b)(s+c)}}ds \tag{46-b}$$

$$N_{i3} = \frac{abc}{2}\int_{0}^{\infty}\frac{1}{(s+c)\sqrt{(s+a)(s+b)(s+c)}}ds \tag{46-c}$$

For the case of a carbon nanotube inclusion $a = b = r_c$ and c corresponds to the half-length of the carbon nanotube. To simplify the formulation it is assumed that all nanotube inclusions are directed parallel to the z axis. In this case the depolarization effect of the inclusions would be mainly dominating in the z direction while the dielectric constant in transverse directions would be the same as the base dielectric. In this case the dielectric constant of the carbon nanotube inclusion is defined as $\varepsilon_i = j\sigma_{3D}/\omega$ where the equivalent 3D conductivity of carbon nanotube is related to the surface dynamic conductivity of carbon nanotube as $\sigma_{3D} = \pi\sigma_{zz}/2r_c$ (Mikki & Kishk 2009). Different experimental researches have been introduced to study the electrical prosperities of carbon nanotube composites. We demonstrate two specific cases in this following part of this section as examples for these carbon nanotube composites.

In microwave hyperthermia applications, it is required to an increase electromagnetic power dissipation in the specific region that is required to be more heated than other regions. Carbon nanotubes are found to be a good candidate for this application. To verify the applicability of carbon nanotube in this application (Mashal *et al.* 2010) demonstrated an experiment based on mixing tissue mimicking materials with carbon nanotubes and measuring their electrical properties and their heating response to incident electromagnetic wave. These tissue mimicking materials are constructed from oil-in-gelatin dispersions. The dielectric properties of these materials are customized to mimic the properties of a variety of human soft tissues by controlling the concentrations of gelatin, safflower oil, kerosene, and preservatives. The carbon nanotubes used in their experiments were 1-2 nm in diameter and 5-30 μm in length, and were composed of mainly single wall carbon nanotubes. Figure 14 shows the measured relative permittivity and effective conductivity of the corresponding composite for different concentrations of carbon nanotubes. It can be noted that both the permittivity and effective conductivity of the tissue mimic materials increase by increasing concentration of the carbon nanotubes.

The electromagnetic heating responses of this tissue mimic composites with carbon nanotube were examined by inserting a sample inside a WR-284 rectangular wave guide of an inner cross section 72 mm × 34 mm and applying a 3-GHz CW signal of power 1 Wt. The source generator is turned on for 3 minutes to heat the sample and turned off for 5 minutes to cool the sample. Figure 15 shows the measured heating responses for different values of carbon nanotube concentrations. It can be noted that the maximum temperature of the tissue mimic mixture increases by increasing the concentration of carbon nanotubes.

It can be concluded from these results that low concentrations of carbon nanotubes significantly impact the dielectric properties and heating response of tissue mimicking materials. For example, at 3 GHz, carbon nanotubes concentrations as small as 0.22% by weight increased the relative permittivity of the tissue mimicking material by 37% and the effective conductivity by 81%. This concentration of carbon nanotubes led to an average steady-state temperature rise that was 6 $^{\circ}$C higher than the rise observed in the tissue mimicking material without carbon nanotubes. These results suggest that carbon nanotubes may enhance contrast for microwave imaging and facilitate selective microwave heating for treatment of breast cancer (Mashal *et al.* 2010).

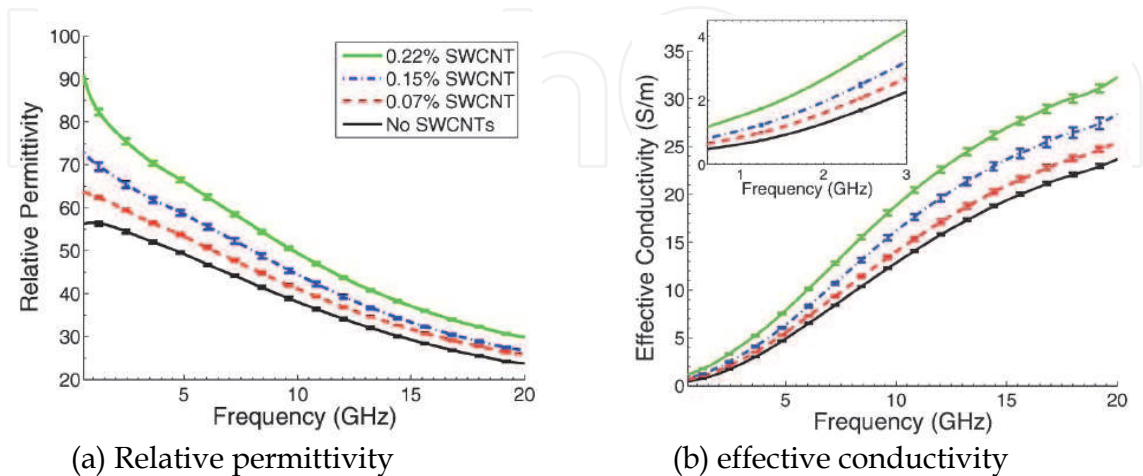(a) Relative permittivity   (b) effective conductivity

Fig. 14. Electrical properties of tissue-mimicking mixtures with varying concentrations of single wall carbon nanotubes measured from 0.6 to 20 GHz. (Mashal *et al.* 2010)
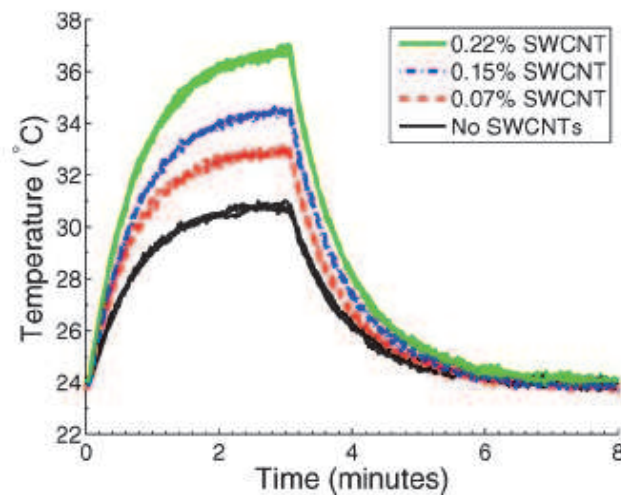
Fig. 15. Microwave heating response of tissue mimic materials with various concentrations of carbon nanotubes. Each curve shows the temperature profile of a sample that was heated via 3-GHz microwave illumination for 3 min and allowed to cool for 5 min. (Mashal *et al.* 2010)

Another important application of carbon nanotube composites is optical-transparent electromagnetic shielding composite film. Thin films of conducting single wall carbon nanotube of a thicknesses less than 300 nm on polyethylene terephthalate substrates are good candidate for this application. (Xu *et al.* 2007) introduced an experimental study to characterize the shielding properties of these composite films. Their study is based on measuring the reflection coefficient of a coaxial annular ring resonator placed above the carbon nanotube layer by using a vector network analyzer. Based on this reflection coefficient they obtained the equivalent impedance of the composite film. This impedance includes the impedance of the carbon nanotube film and the impedance of the holding substrate. To extract the impedance of the substrate, they measured the reflection coefficient of the coaxial annular resonator on the substrate only. After extracting the impedance of the substrate, they obtained the impedance of the carbon nanotube layer. This impedance is used to determine the equivalent complex conductivity of the carbon nanotube layer. Then the problem is treated as a two-layered structure of specific values of permitivities and conductivities to determine the transmission coefficient of this structure.

Figure 16 shows the shielding effectiveness in dB as a function of frequency for different thicknesses of carbon nanotube films. It is noted that this shielding effectiveness is proportional to $\log (1/f)$. For the 10 nm film, the shielding effectiveness varies from 43 to 28 dB in the range of 10 MHz–30 GHz. The dependence of the shielding effectiveness on the thickness of the carbon nanotube layer t_0 is nearly proportional to $\log (t_0)$. On the other hand, Figure 17 shows the optical transmission coefficient at wavelength of 550 nm as a function of the thickness of the carbon nanotube film. For a 30 nm thickness film, the optical transmittance is about 80% and the shielding effectiveness are 33 dB at 10 GHz, 36 dB at 1 GHz, and 46 dB at 10 MHz. This shielding effectiveness of carbon nanotube films satisfies requirements for commercial applications like cell phones which require approximately 20 dB shielding effect. For high shielding requirements such as for magnetic resonant imaging window where 60 dB shielding effectiveness is required, carbon nanotube films still need to be improved.
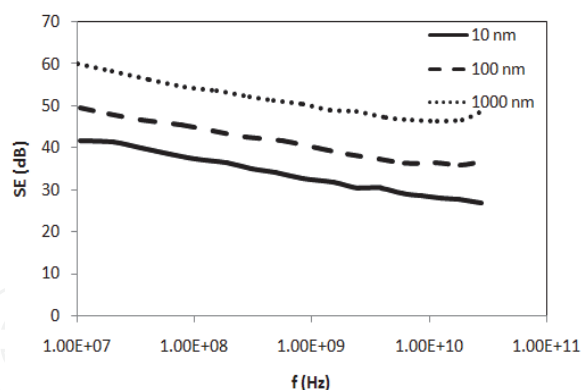
Fig. 16. Microwave shielding effectiveness of a carbon nanotube film for different values of thicknesses. (Xu *et al.* 2007)
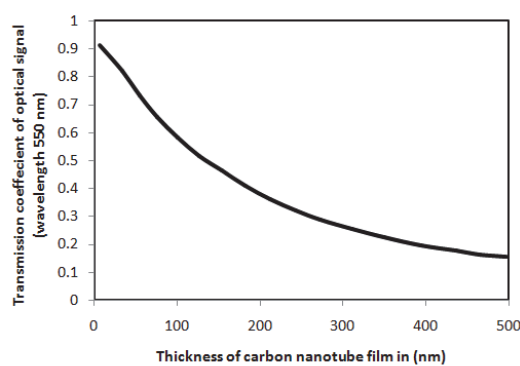

Fig. 17. Optical transmission coefficient at wavelength of 550 nm as a function of the thickness of carbon nanotube film. (Xu *et al.* 2007)

9. Conclusion

This chapter introduced different techniques for studying interaction of high frequency electromagnetic fields with carbon nanotubes. Boltzman kinetic equation is used to introduce an equivalent surface conductivity and electron fluid model is used to introduce an equivalent circuit model for carbon nanotube transmission line. Another model is introduced based on coupling Maxwell's equation with Schrodinger equation. Finite difference time domain is discussed as an efficient numerical technique for solving coupled Maxwell-Schrodinger equations to obtain a full wave analysis for electromagnetic interaction with carbon nanotubes.

These models show that carbon nanotubes are characterized by high inductive effect due to the additional kinetic inductance. This high inductive effect reduces wave velocity along carbon nanotubes and increases its corresponding characteristic impedance. Reduction of wave velocity has a significant importance in reducing the size of RF components, passive circuits and antenna structures. On the other hand, parallel carbon nanotubes can be used to reduce the characteristic impedance. Analytical analysis of surface wave propagation along circular carbon nanotube bundle is discussed based on the equivalent surface conductivity. Resulting complex wave propagation constant along carbon nanotube bundles shows slow wave propagation which is consistent with the transmission line model introduced by

electron fluid model. In addition, attenuation coefficient is found to be increased by decreasing the operating frequency. Carbon nanotubes are also found to be a good candidate for dipole antennas at operating frequencies above 100 GHz. At lower frequencies the high attenuation coefficient of wave propagation along the carbon nanotube structure makes it not suitable to obtain resonant antenna. Further theoretical and experimental studies are still required to investigate the possibility of using parallel carbon nanotubes in RF circuits and antennas. In addition electro-mechanical properties of carbon nanotubes can be also be useful in RF applications like filtering and switching. On the other hand, the high attenuation at lower frequencies below 100 GHz makes carbon nanotubes good candidate for absorbing and shielding applications. Absorbing properties of carbon nanotubes can be quite useful in medical applications such as microwave imaging and selective microwave heating for cancer treatment. Thin film of carbon nanotubes above a polyethylene substrate is also found to good candidate for transparent shielding surface up to 20dB. Higher shielding effectiveness combined with high transparence is still under investigation.

10. Acknowledgement

11. References

Ahmed, I.; Khoo, E. H.; Li, E. & Mittra, R. (2010). A hybrid approach for solving coupled Maxwell and Schrödinger equations arising in the simulation of nano-devices. *IEEE Antenna and Wireless Propagations Letters*, Vol. 9, (2010), pp. 914-917

Attiya, A.M. (2009). Lower frequency limit of carbon nanotube antenna. *Progress In Electromagnetics Research*, Vol. 94, 419-433, 2009.

Attiya, A.M.; Alkanhal, M.A. (2009). Parallel single wall carbon nanotubes for microwave applications. *Microwave Conference, 2009. APMC 2009. Asia Pacific*, 7-10 Dec. 2009, pp.2459-2462

Burke, P. J. (2002). Lüttinger Liquid Theory as a Model of Gigahertz Electrical Properties of Carbon Nanotubes. *IEEE Trans. Nanotechnology*, Vol. 1, No.3, (Sept. 2002), pp. 129-144

Chiariello, A.G.; Maffucci, A.; Miano, G.; Villone, F.; Zamboni, W. (2006a). Metallic Carbon Nanotube Interconnects, Part I: a Fluid Model and a 3D Integral Formulation," *IEEE Workshop on Signal Propagation on Interconnects*, 9-12 May 2006, pp.181-184

Chiariello, A.G.; Maffucci, A.; Miano, G.; Villone, F. & Zamboni, W. (2006b). Metallic Carbon Nanotube Interconnects, Part II: a Transmission Line Model. *IEEE Workshop on Signal Propagation on Interconnects*, 9-12 May 2006, pp.185-188

Demoustier, S.; Minoux, E.; Baillif,M. L.; Charles,M.; and Ziaei,A. (2008), Review of two microwave applications of carbon nanotubes: nano-antennas and nano-switches, *Comptes Rendus Physique*, Vol. 9, No. 1, *New concepts for nanophotonics and nano-electronics*, (Jan. 2008), pp. 53-66

Dragoman, M., Hartnagel, H. L.; Tuovinen, J; and Plana, R. (2005), Microwave applications of carbon nanotubes, *Frequenz*, Vol. 59 No. 11-12, (2005) pp. 251-263

Dressel, M. & Grüner, G. (2003). *Electrodynamics of Solids: Optical Properties of Electrons in Matter*, Cambridge University Press, ISBN 0 521 59253 4, Australia

Elliot, R. S. (2003). *Antenna theory and design*, IEEE press, ISBN 0471449962.

Hanson, G. W. (2005). Fundamental Transmitting Properties of Carbon Nanotube Antennas. *IEEE Trans. Antennas Propag.*, Vol. 53, No. 11, (Nov. 2005), pp. 3426-3435

Hanson, G. W. (2006). Current on an infinitely-long carbon nanotube antenna excited by a gap generator. *IEEE Trans. Antennas Propag.*, Vol. 54, No. 1, (Jan. 2006), pp. 76-81

Hao, J. & Hanson, G. W. (2006). Infrared and Optical Properties of Carbon Nanotube Dipole Antennas. . *IEEE Trans. Nanotechnolgy*, Vol. 5, No.6, (Nov. 2006), pp. 766-775

Huang, Y.; Wen-Yan, Y. & Liu; Q. H. (2008). Performance Prediction of Carbon Nanotube Bundle Dipole Antennas. *IEEE Trans. Nanotechnology*, Vol. 3, No.3, (May 2008), pp. 331-337

Koledintseva, M. Y.; Drewniak, J. L.; DuBroff, R. E.; Rozanov, K. N.; & Archambeault, B. (2009), Modeling of shielding composite materials and structures for microwave frequencies, *Progress In Electromagnetics Research B*, Vol. 15,(2009) pp. 197-215

Li, S.; Yu, Z.; Rutherglen, C.; & Burke, P. (2007). Electrical properties of 0.4 cm long single walled carbon nanotubes. *Nano Lett.*, Vol. 4, No. 10, (2007), pp. 2003-2007

Maffucci, A.; Miano, G. & Villone, F. (2009). A New Circuit Model for Carbon Nanotube Interconnects With Diameter-Dependent Parameters. *IEEE Trans. Nanotechnology*, Vol.8, No.3, (May 2009), pp.345-354

Maffucci, A.; Miano, G.; Villone, F. (2008). Electromagnetic and circuital modeling of carbon nanotube interconnects. *Electronics System-Integration Technology Conference, 2008. ESTC 2008. 2nd* , pp.1051-1056, 1-4 Sept. 2008

Mashal, A.; Sitharaman, B.; Xu Li; Avti, P.K.; Sahakian, A.V.; Booske, J.H. & Hagness, S.C. (2010). Toward Carbon-Nanotube-Based Theranostic Agents for Microwave Detection and Treatment of Breast Cancer: Enhanced Dielectric and Heating Response of Tissue-Mimicking Materials. *IEEE Transactions on Biomedical Engineering,* Vol.57, No.8,(Aug. 2010), pp.1831-1834

Massoud, Y. ; & Nieuwoudt, A. (2006). Modeling and Design Challenges and Solutions for Carbon Nanotube-based Interconnect in Future HighPerformance Integrated Circuits. *ACM Journal on Engineering Technologies in Computing Systems*, Vol. 2, No. 3, (July 2006), pp. 155-196

Miano, G. &Villone, F.; (2006). An Integral Formulation for the Electrodynamics of Metallic Carbon Nanotubes Based on a Fluid Model. *IEEE Trans. Antennas Propag.*, Vol.54, No.10, (Oct. 2006), pp.2713-2724,

Mikki, S.M. & Kishk, A.A. (2009). Mean-Field Electrodynamic Theory of Aligned Carbon Nanotube Composites. *IEEE Trans. Antennas Propag.*, Vol.57, No.5,(May 2009), pp.1412-1419

Miyamoto, Y.;Rubio, A.; Louie, S. G.; & Cohen, M. L. (1999). Self-inductance of chiral conducting nanotubes. *Phys. Rev. B*, Vol. 60, No. 19, (Nov. 1999), pp. 13885-11889

Naeemi, A. & Meindl, J. D., (2009). Performance Modeling for Carbon Nanotube Interconnects, In : *Carbon Nanotube Electronics*, Javey, A. ; & Kong, J. (Eds.) 163-189, Springer, ISBN 978-0-387-36833-7

Pierantoni, L.; Mencarelli, D.; Rozzi, T. (2008). A New 3-D Transmission Line Matrix Scheme for the Combined SchrÖdinger–Maxwell Problem in the Electronic/ Electromagnetic Characterization of Nanodevices. *IEEE Transactions Microwave Theory and Techniques*, Vol.56, No.3,(March 2008), pp.654-662

Pierantoni, L.; Mencarelli, D. & Rozzi, T. (2009). Boundary Immittance Operators for the SchrÖdinger–Maxwell Problem of Carrier Dynamics in Nanodevices. *IEEE Transactions Microwave Theory and Techniques*, Vol.57, No.5, (May 2009). pp.1147-1155

Plombon, J. J.; O'Brien, K. P.; Gstrein, F.; Dubin, V. M. & Jiao, Y. (2007). High-frequency electrical properties of individual and bundled carbon nanotubes. *Phys. Lett.* Vol. 90, (2007), pp. 063106

Rutherglen, C.; Jain, D. & Burke, P. (2008). RF resistance and inductance of massively parallel single walled carbon nanotubes: Direct, broadband measurements and near perfect 50 Ω impedance matching. *Appl. Phys. Lett.* Vol .93,(2008), pp. 083119

Shuba, M. V.; Maksimenko, S. A. & Lakhtakia, A. (2007). Electromagnetic wave propagation in an almost circular bundle of closely packed metallic carbon nanotubes. *Physical Review B*, Vol. 76, (2007), 155407

Slepyan, G. Y.; Maksimenko, S.A.; Lakhtakia, A.; Yevtushenko, O. M. & Gusakov, A. V. (1998) Electronic and electromagnetic properties of nanotubes, *Physical Review B*, Vol 57, No. 16 (April 1998), pp. 9485-9497

Slepyan, G. Y.; Maksimenko, S. A.; Lakhtakia, A.; Yevtushenko, O. & Gusakov, A. V. (1999). Electrodynamics of carbon nanotubes: Dynamic conductivity, impedance boundary conditions, and surface wave propagation. *Physical Review B*, vol. 60, Issue 24, (1999), pp. 17136-17149

Slepyan, G. Ya.; Nemilentsau, A. M. & Maksimenko, S. A. (2008). Electromagnetic Theory of Nanodimensional Antenna for Terahertz, Infrared and Optics Regiems. *2008 12th International Conference on Mathematical Methods in Electromagnetic Theory*, June 29-July 02, pp. 118-123, Odesa, Ukraine

Xu, H.; Anlage, S. M.; Hu, L. & Gruner, G. (2007). Microwave shielding of transparent conducting single-walled carbon nanotube films. *Applied Pysics Letters*, Vol. 90, (2007), 183119

Carbon Nanotubes Applications on Electron Devices

Edited by Prof. Jose Mauricio Marulanda

Carbon nanotubes (CNTs), discovered in 1991, have been a subject of intensive research for a wide range of applications. In the past decades, although carbon nanotubes have undergone massive research, considering the success of silicon, it has, nonetheless, been difficult to appreciate the potential influence of carbon nanotubes in current technology. The main objective of this book is therefore to give a wide variety of possible applications of carbon nanotubes in many industries related to electron device technology. This should allow the user to better appreciate the potential of these innovating nanometer sized materials. Readers of this book should have a good background on electron devices and semiconductor device physics as this book presents excellent results on possible device applications of carbon nanotubes. This book begins with an analysis on fabrication techniques, followed by a study on current models, and it presents a significant amount of work on different devices and applications available to current technology.

How to reference

In order to correctly reference this scholarly work, feel free to copy and paste the following:

Ahmed M. Attiya and Majeed A. Alkanhal (2011). Carbon Nanotubes in Passive RF Applications, Carbon Nanotubes Applications on Electron Devices, Prof. Jose Mauricio Marulanda (Ed.), ISBN: 978-953-307-496-2, InTech, Available from: http://www.intechopen.com/books/carbon-nanotubes-applications-on-electron-devices/carbon-nanotubes-in-passive-rf-applications

INTECH
open science | open minds